New Prediction Formula of Fourier Spectra Based on Separation Method of Source, Path, and Site Effects Applied to the Observed Data in Japan

Kenichi Nakano
Graduate School of Engineering, Kyoto University, Kyoto, Japan

Hiroshi Kawase
DPRI, Kyoto University, Uji, Kyoto, Japan

Shinichi Matsushima
DPRI, Kyoto University, Uji, Kyoto, Japan

SUMMARY:
The objective of this study is to predict Fourier and response spectra based on a generalize spectral inversion method of source, path, and site effects applied to the observed data by K-NET, KiK-net, and JMA Shindokei (Seismic Intensity measurement) Network in Japan. The separation method we used here was the same method proposed by Kawase and Matsuo (2004). In this study, first we obtain source, path, and site terms using the separation method mentioned above. Here we include all the sources larger than Mj4.5 from 1996 to 2011, effectively included numbers of aftershocks of the Off the Pacific Coast of Tohoku earthquake (yet excluding the main shock because of pervasive nonlinear site effects), in total about twice as much as the sources used by Kawase and Matsuo (2004). After the separation then we compared the resultant source, path, and site characteristics with those obtained by Kawase and Matsuo (2004). We found that basic features of source and path characteristics between these two analyses are quite similar, although we can see apparent differences in the stress parameters for crustal earthquakes. In our second phase of analyses, we will repeat the same analysis for response spectra in order to compare separated quantities of response spectra with those of Fourier spectra and to compare resultant response spectra attenuation function with attenuation functions proposed in previous studies.

Keywords: Response spectra, Spectral inversion, Seismic moment, Stress drop, S-wave velocity

1. INTRODUCTION

The objective of this study is to predict Fourier and response spectra based on a generalize spectral separation method of source, path, and site effects applied to the observed data by K-NET, KiK-net, and JMA Shindokei (Seismic Intensity measurement) Network in Japan. Adequate evaluation of the strong motion characteristics is indispensible for quantitative strong motion prediction. Empirical strong motion prediction methodology has been studied extensively by engineers as attenuation function (or Ground Motion Prediction Equations, i.e., GMPE) construction based on pre-defined regression formula (e.g., Boore and Atkinson, 2008, Scasserra et al., 2009, or Kanno et al., 2006). On the other hand, separation of source, path, and site effects in terms of Fourier spectra of observed data has been widely performed by using the generalized spectral inversion technique in seismology (e.g., Andrews, 1982). These separated quantities can be used to reproduce artificial seismograms suitable for the statistical Green's function method (e.g., Kawase et al., 2000). However, the study on response spectra using such a separation method seems quite rare primarily because response spectra are considered to be different from Fourier spectra, which have a clear physical meaning appropriate to separate three basic quantities. It turns out that, however, response spectra share the similar characteristics to Fourier spectra so that it is worth to try to predict response spectra at each site by using a method of spectral separation.

Response spectra clearly show relationship between natural period of building and predominant period of seismic motions. Response spectra are used as one of the significant indicator to determine seismic input to design a structure. Thus it is desirable if we can predict directly and precisely a response spectrum due to a specific source at a specific site for the engineering purpose.

The separation method we used here was the one proposed by Kawase and Matsuo (2004). They carried out separation of source, path, and site characteristics using the generalized inversion technique based on the observed data of K-NET, KiK-net, and the JMA Shindokei network in Japan with one reference hard-rock site whose S-wave velocity is considered to be 3.4km/s. They applied the same technique not only to observed Fourier spectra but also Peak Ground Acceleration (PGA) and Peak Ground Velocity (PGV) successfully. Since PGA and PGV are indexes of the peak values as are response spectra, we can expect the same method can also be applied to response spectra.

In the first stage of analysis we perform the same spectral inversion as Kawase and Matsuo (2004) for Fourier spectra by using larger numbers of observed data. After the separation we got site factors with some significant differences from those of Kawase and Matsuo (2004). Therefore we extensively check the validity of our calculation before applying the same technique to response spectra.

2. DATASET AND METHOD OF ANALYSIS

We use K-NET, KiK-net, and JMA Shindokei network as source of strong ground motion data in Japan. K-NET started in operation from May 1996 with 1,000 surface stations, while KiK-net started in operation from June 1997 with about 500 surface and downhole stations (at present 692 stations). K-NET stations have P-S logging velocity profiles up to 20 m, while KiK-net stations have those up to the depths of downhole stations, usually 100 m to 200 m, except for 21 sites inside sedimentary basins for which we have more than 1,000 m in depth. We also use strong ground motion data from the JMA Shindokei network, which was designed to quickly broadcast JMA seismic intensity, and started in operation from October 1996. JMA stations do not have any information on their site conditions, yet.

Recently, social demands of the effective use of these strong ground motion record are getting increasing (e.g., We had "the Off the West Coast of Northern Sumatra of M_W9.0 earthquake" on December 2004 in Indonesia, "The Christchurch earthquake of M_L6.3" on February 2011 in New Zealand, and "The Off the Pacific Coast of Tohoku earthquake of Mw9.0" on March 2011 in Japan). Thus we need to consider how to use these data for engineering purposes. This study is one of the attempts for effective use of these data.

We first make a dataset for spectral inversion of this study. The dataset is consists of two horizontal component records of strong ground motions with the condition of i) $M_{jma} \geq 4.5$, ii) the focal depth $\leq$ 60 km, iii) the hypocentral distance $\leq$ 200 km, and iv) the peak ground acceleration $\leq$ 200 Gals recorded by K-NET, KiK-net, JMA Shindokei network in Japan from January 2004 to December 2011, except for the main shock of the Tohoku earthquake (M_{jma}9.0) because of its extraordinary features in every aspects of the source and ground motion characteristics. After scrutiny we found that the data used consists of 42,286 source-station pairs and 352 earthquakes, approximately twice of Kawase and Matsuo (2004). The sites where these data were recorded are shown in Fig. 2.1(a) by yellow circles. The numbers shown in each region divided by thin lines are region numbers that account for regional difference in attenuation characteristics.

We can divide 352 earthquakes into these three categories, namely, the plate boundary earthquakes Type B (in total 176), the intraplate earthquakes, Type I (92), and the crustal earthquakes, Type C (84). Fig.2.1 (b), (c), and (d) shows the locations and mechanism solutions of earthquakes used this study for each category. Source locations are those of JMA (JMBSC, 2011, it is published at http://www.jmbsc.or.jp/english/index-e.html) and mechanism solutions are those from CMT solution by F-NET (NIED, 2011, it is published at http://www.fnet.bosai.go.jp/top.php?LANG=ja).

To analyze data, first we cut out the target accelerograms from the onset of S-wave with the duration of 5 seconds (M<6), 10 seconds (M<7), or 15 seconds (M>7) in order to restrict ourselves to analyze only S-wave portion of incident waves. We use the standard travel-time table used by JMA, and we confirmed visually that it works quite well for most of the cases. Then, we calculate the Fourier spectra of these accelerograms.

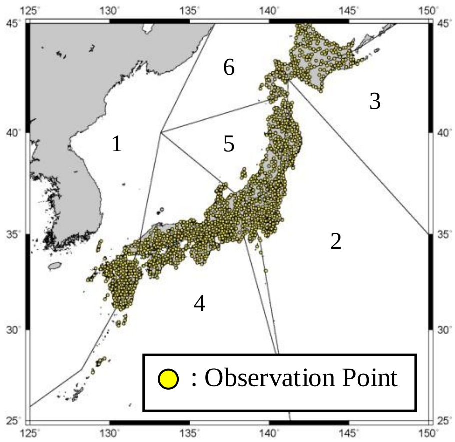

(a) The observation point and divided area in Japan

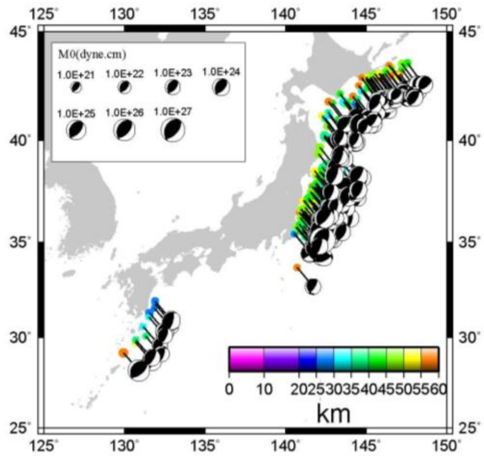

(b) The boundary earthquakes

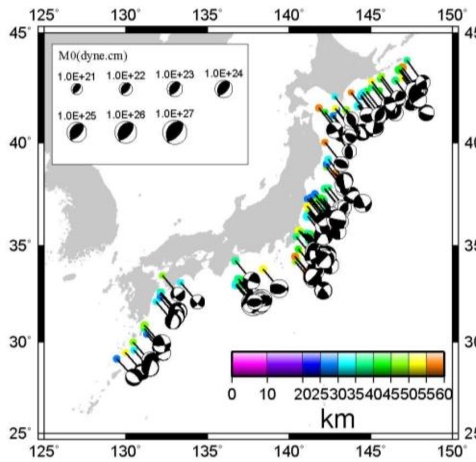

(c) The intraplate earthquakes

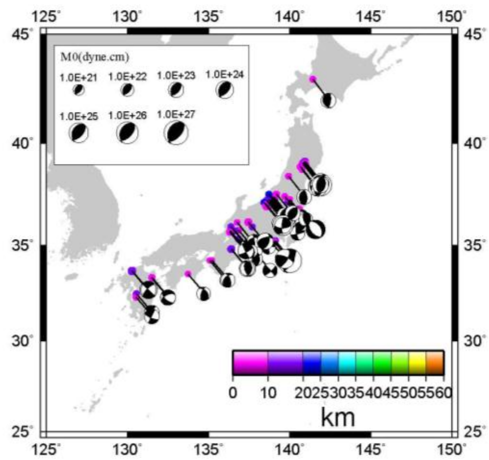

(d) The crustal earthquakes

Figure 2.1. The observation point and the locations and mechanisms of earthquakes used

For Fourier spectra *Fij* for i-th earthquake observed at j-th site, we use the following equation:

$$\log F_{ij} = \log S_i - n_{l(i)} \log X_{ij} + \sum_k b_{l(i)k} X_{ijk} + \log G_j \tag{2.1}$$

$$X_{ij} = \sum_k X_{ijk} \tag{2.2}$$

where, S_i is the source spectrum for *i*-th earthquake, G_j is the site factor for *j*-th site, X_{ij} is the direct hypocentral distance for that pair, *k* is a region number with different attenuation as shown in Fig. 2.1(a), *l*(*i*) is source type (B, I, or C). These Eqn. 2.1 and 2.2 are the same equations of Kawase and Matsuo (2004) or Kawase (2006). We use both parameters for geometrical spreading *n* and intrinsic and scattering attenuation *b*. To delineate different attenuation characteristics at different regions in Japan, we divide Japan into six regions, as shown in the Fig. 2.1(a), in which we assume a different attenuation coefficient *b*. We also assume that these parameters *n* and *b* are source-type dependent. The reason why we introduce *n* as a separate parameter for geometrical spreading is to explain small attenuations in the intermediate distance range for shallow crustal earthquakes. We assume constant *n* equal to 1 for distance from 0 to 100 km.

3. COMPARISON OF RESULT OF SPECTRAL INVERSION

We perform the separation of variables by using spectral inversion method for the dataset mentioned above. The obtained results are different from previous studies because of different dataset used.

Especially, Site factors estimated by spectral inversion in this study and those by Kawase and Matsuo (2004) are significantly different. The differences of site factors for K-NET sites are more remarkable than site factors for KiK-net. Thus we have to investigate the source of differences in the calculation of spectral inversion in this study. We compare here site factors, Q factors, seismic moments, M0-Fc and M0-Fmax relationships, and stress drop distributions in these studies.

3.1. Site Factor

Kawase and Matsuo (2004) used a site YMGH01 (KiK-net) as the reference site of spectral inversion. Kawase (2006) also used the same location as in Kawase and Matsuo (2004). This site has three layers whose S-wave velocity are 1,000 m/s, 2,100 m/s, and 3,100m/s according to the S-wave velocity structure by P-S logging (NIED, it is published at http://www.kyoshin.bosai.go.jp/). The site factor used by Kawase and Matsuo (2004) and Kawase (2006) is estimated by using the Genetic Algorithm (GA) to match the phase difference and spectral ratio between surface and downhole records to the corresponding values computed by 1-D theory at YMGH01. After looking all the site factors obtained as relative amplification factors with respect to YMGH01, we found a few site with smaller site factors (i.e., less than 1.0) in our target frequency range of 0.3 Hz to 20 Hz. However, we could not find any site with sufficient numbers of data with the bedrock velocity higher than 3.0 km/s. So we also select YMGH01 as the reference site of our spectral inversion.

Fig. 3.1 (a), (b), and (c) show site factors (amplification factors) at MYG004, CHB008, and IBRH11 as examples. Blue lines show site factors of Kawase and Matsuo (2004), red lines show site factors of this study (as Nakano), black lines show the average of site factors determined by individual site factor estimates, and black dash lines show the average$\pm\sigma$. Other lines are of individual site factors back calculated by extracting source and path effects from the observed spectra. The site factors seem to be properly calculated by our spectral inversion because red lines are within the range of average$\pm\sigma$. However, in Fig. 3.1(a) and (b), blue lines are not within the range of average$\pm\sigma$. In contrast, in Fig. 3.1(c), a blue line is within the range of average$\pm\sigma$ and in good agreement with the red line. Since theoretically it is impossible to have the same site factors at some sites and at the same time different site factors at other sites in one spectral inversion, resultant site factors with significant difference such as those shown in Fig. 3.1(a) and (b) suggests that increased numbers of data at these sites may contribute to reduce their average site factors as shown here.

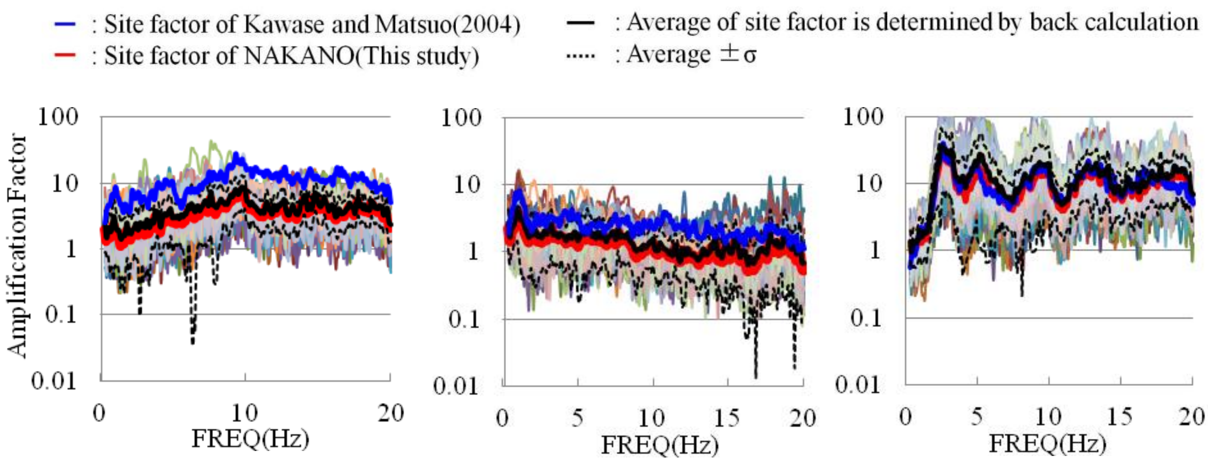

(a) Site factor of MYG004 (b) Site factor of CHB008 (c) Site factor of IBRH11

Figure 3.1. Comparison of site factors at three example sites

3.2. Attenuation Q-1 and Intrinsic and Scattering Attenuation b Value

Q value is an index of decreasing energy per unit travel length and can be calculated from *b* value due to wave propagation through to the propagation path. In our inversion *b* value is the attenuation coefficient that reflects both internal (intrinsic) attenuation and scattering attenuation. Q value is obtained from *b* value using Eqn. 3.1 for 1/Q.

$$ {}^{1}/_{Q(f)} = \frac{-b(f) \cdot Vs \cdot \ln 10}{\pi \cdot f} \tag{3.1} $$

Fig. 3.2 shows comparison of 1/Q and *b* values for regions from 1 to 6 shown in Fig. 2.1. In Fig. 3.2, top panels are for 1/Q and bottom ones are for *b* values for each earthquake type; namely, (a) and (d) are for plate boundary earthquakes Type B, (b) and (e) are for intraplate earthquakes Type I, and (c) and (f) are for crustal earthquakes Type C. Note that for Type C earthquakes, Kawase and Matsuo (2004) has only 4 results (the region 1, 2, 4, 5) because of too less data and so unstable results. In all the figures, blue lines show region 1, green lines show region 2, red lines show region 3, yellow lines show region 4, black lines show region 5, and purple lines show region 6. Among them solid lines show results of this study (Nakano), and dotted line show those of Kawase and Matsuo (2004). Clearly, 1/Q and *b* values of this study show more stable characteristics compared to those of Kawase and Matsuo (2004). This would be due to increased numbers of data. Especially, in Fig. 3.2 (a) and (b), the solid purple lines are much more stable than the dotted purple lines. On the other hand, the solid lines are very close to the dotted lines in the region and in the frequency range where dotted lines show smaller fluctuations. Thus it suggests that our results do better represent the real attenuation characteristics in each region and in each earthquake category thanks to plenty of data used in the inversion.

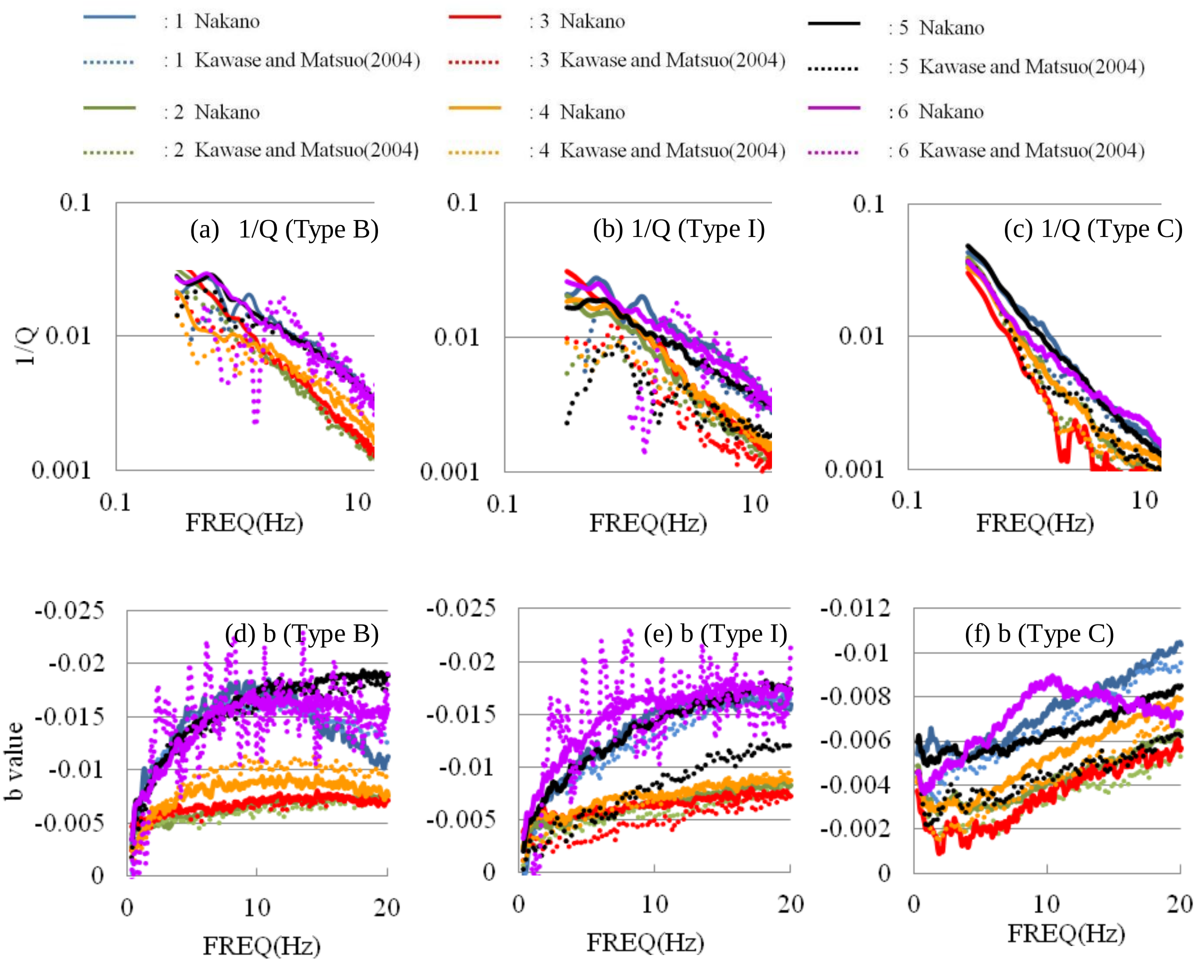

Figure 3.2. 1/Q and b values for each region and each earthquake category

The 1/Q of the intraplate earthquakes and the boundary earthquakes are slightly bigger than the 1/Q of the crustal earthquakes. This tendency agrees with the previous study. Although a little hard to see because lines are overlapping, blue lines (region 1 in Fig. 2.1 (a)) show the largest attenuation regardless of the type of earthquakes. We should note here that the values of 1/Q obtained in this study are the average one for each region. These tendencies were also supported by the result of Kawase and Matsuo (2004).

3.3. M0-fc and M0-fmax Relation

M0 here is called the seismic moment that is the most fundamental source parameter that we can use to measure the size of an earthquake caused by a fault slip (Aki and Richards, 2009). We use the seismic moment published by Full Range Seismograph Network of Japan (F-NET) of NIED (it is published by http://www.fnet.bosai.go.jp/top.php?LANG=en) for almost all the earthquakes we used, except for some earthquakes whose values have not been published. If not, we also determined M0 by fitting the theoretical prediction to the inverted source spectra. We calculate f_{max} and f_c using the same method as Kawase and Matsuo (2004), where f_c is a corner frequency, while f_{max} is a cut-off frequency.

Fig. 3.3 shows the relationships of M0-fc (upper figure) and M0-fmax (lower figure) for each earthquake types. Blue squares show relationships of Kawase and Matsuo (2004) while red circles show those of our study (as shown Nakano). We also plot the regression lines in all the figures, for Kawase and Matsuo (2004) by dotted lines and this study by solid lines, respectively. R-square (R2) is called coefficient of determination. If the value of R2 is near to 1.0, the prediction capability is high. In contrast, if the value of R2 is near to 0, the prediction capability is low. In the case of former, it means that data has strong correlation, while in the case of latter, it means that data has no correlation.

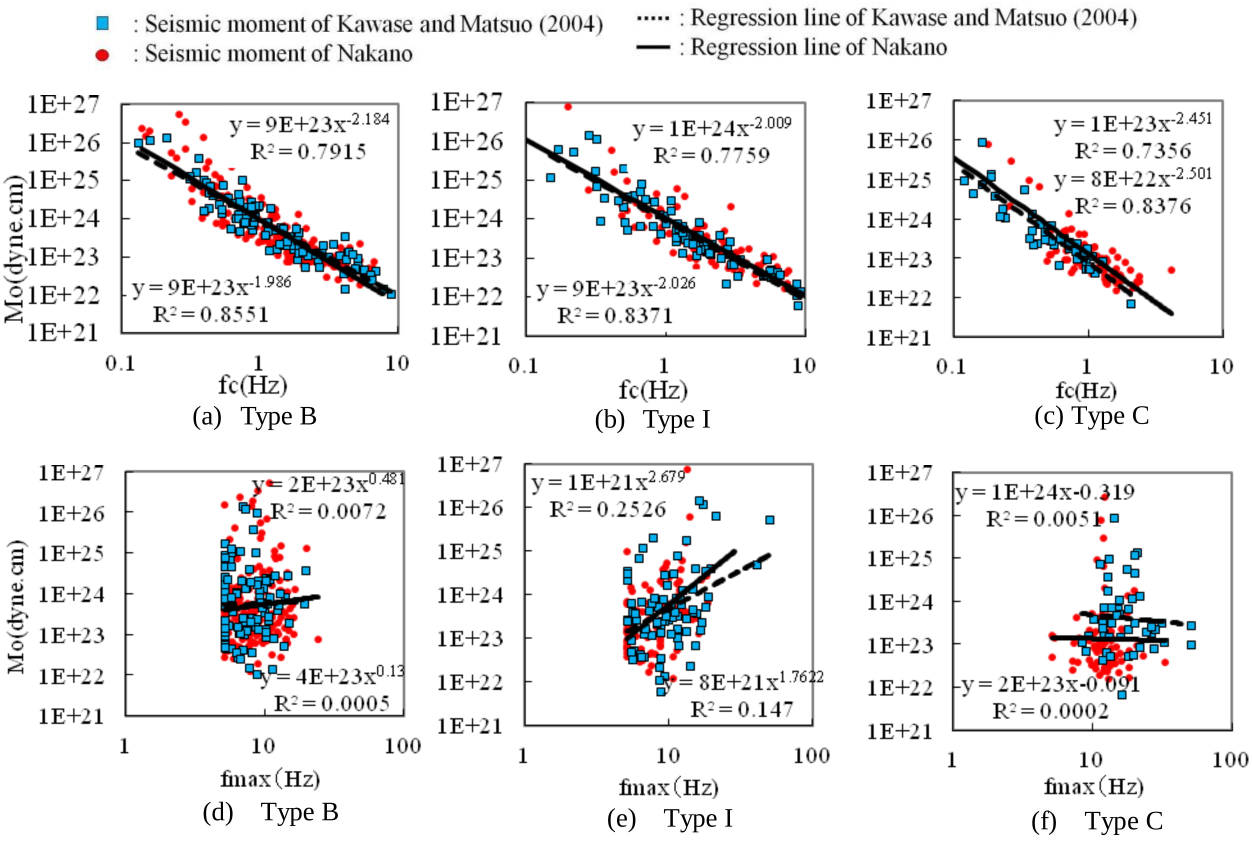

Figure 3.3. M0-fc and M0-fmax relationships for each earthquake category

In all the figures, the regression lines for Kawase and Matsuo (2004) and this study (Nakano) match quite well. Especially, Fig. 3.3 (a), (b), (c), and (d) show the very good match between them. However, Fig. 3.3 (e) and (f), f_{max} for the intraplate and crustal earthquakes does not match so well despite the similarity of their tendencies.

3.4. Stress Parameter $\Delta\sigma$ and Seismic Moment M0 Relations

To investigate the scale dependence of earthquakes on stress drops, even though its physical meaning is not always clear, we calculate the so-called Brune's stress drop $\Delta\sigma$ (we call it as stress parameter $\Delta\sigma$ hereafter). We show it in Fig. 3.4 (a), (b), and (c) as a function of the seismic moment. We also show their hypocentral depth dependence in Fig. 3.4 (d), (e), and (f). In Fig. 3.4 (d), (e), and (f), we also show the average of our data (black lines) and the average$\pm\sigma$ (one standard deviation) of our data (dash lines) because depth dependence seems small. These results imply the validity of our results because there are no significant differences in the data distributions between blue boxes (previous study) and red circles (current study). In Fig. 3.4 (a), (b), the scale dependence of the stress parameter (solid lines) is smaller than the previous study (dashed lines). In contrast, in Fig. 3.4 (c), the scale dependence is larger than the previous study. We should note that small linear dependence of the stress parameter is the primary cause of the power of 2 proportional coefficients in M0-fc relationships shown in Fig. 3.2 (a) and (b).

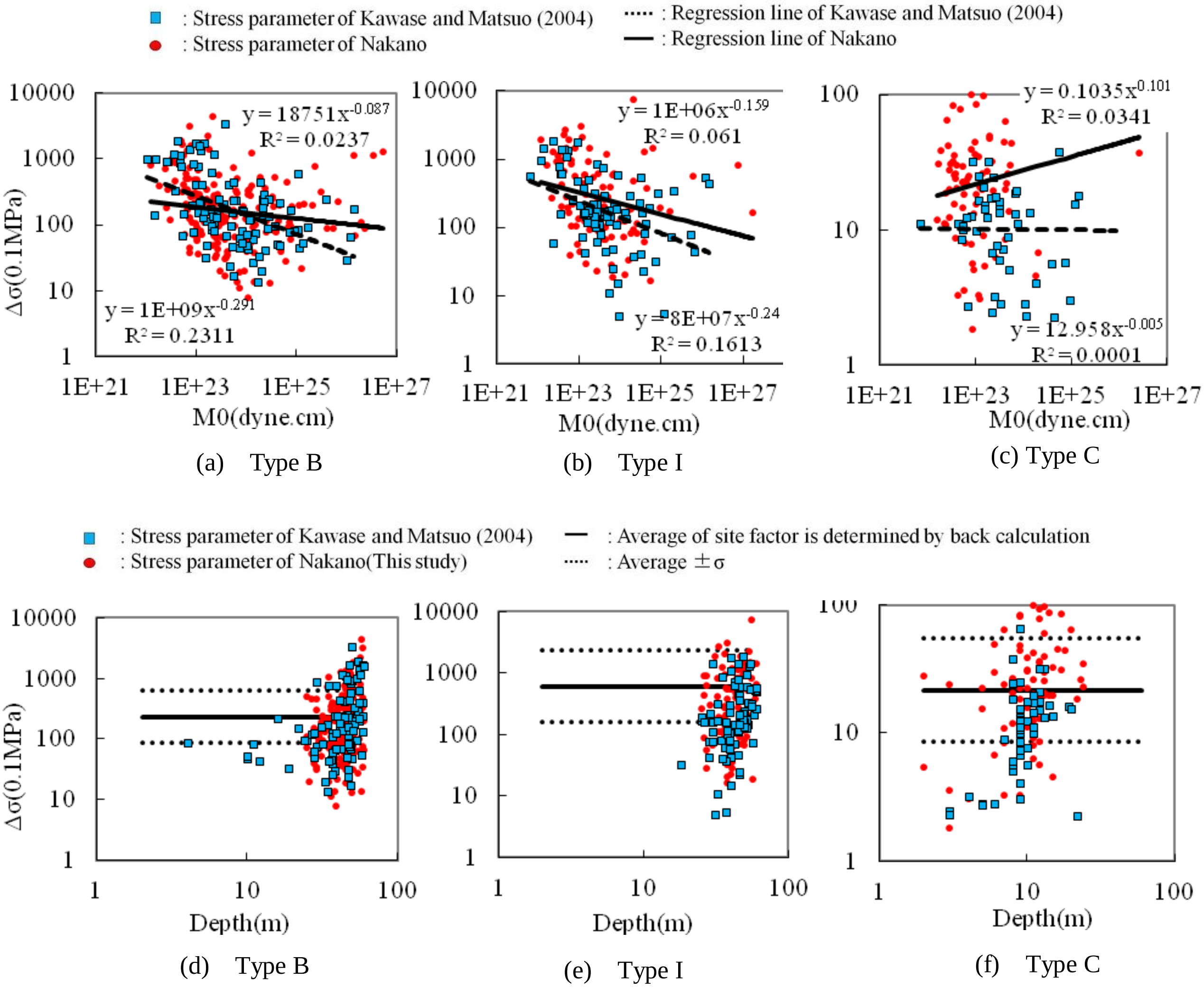

Figure 3.4. Comparison of $\Delta\sigma$-M0 and $\Delta\sigma$-Depth relationships for each earthquake category

4. INVERSION OF S-WAVE VELOCITY STRUCTURE

We identify the S-wave velocity structure that is deeper than the published P-S logging, using the site factors of Fourier spectra estimated by spectral inversion, as to fit the site factors to amplification factors estimated from 1-D wave propagation theory using Genetic Algorithm. We need to determine both the S-wave velocity and layer thickness since they are unknown.

Here we follow the GA procedure of Kawase and Matsuo (2004); we fix the published PS logging data and invert only three layers' parameters, both thickness and S-wave velocity, plus the thickness of the bottommost layer in order to minimize the residual between separated site factors and theoretical 1-D amplification from 0.3Hz to 20Hz. The density of each layer is calculated as a function of S-wave velocity and the same Q of $19f^{0.52}$ was assumed for all the layers to avoid the trade-off between S-wave velocity and damping.

We estimate the S-wave velocity and depth structure for three sites in Japan based on the site factors at these sites (see Fig. 3.1 (a), (b), and (c)). Three sites selected here are MYG004, CHB008, and IBRH11. We show these result in Fig. 4.1 below. Fig. 4.1 (a) shows the S-wave velocity structure at MYG004, Fig. 4.1 (b) shows the S-wave velocity structure at CHB008, and Fig. 4.1 (c) shows the S-wave velocity structure at IBRH11. In all the figures, red lines show the S-wave velocity structures estimated by us (as shown Nakano), blue lines show the S-wave velocity structures estimated previously by Kawase and Matsuo (2004), black lines only in the shallower part show the S-wave velocity structures of the P-S logging obtained by NIED. The S-wave velocities at MYG004 and CHB008 are estimated to be softer than the S-wave velocities of Kawase and Matsuo (2004), while the S-wave velocities at IBRH11 do not show significant differences from those of Kawase and Matsuo (2004) reflecting the similar site factors shown in Fig. 3.1 (c).

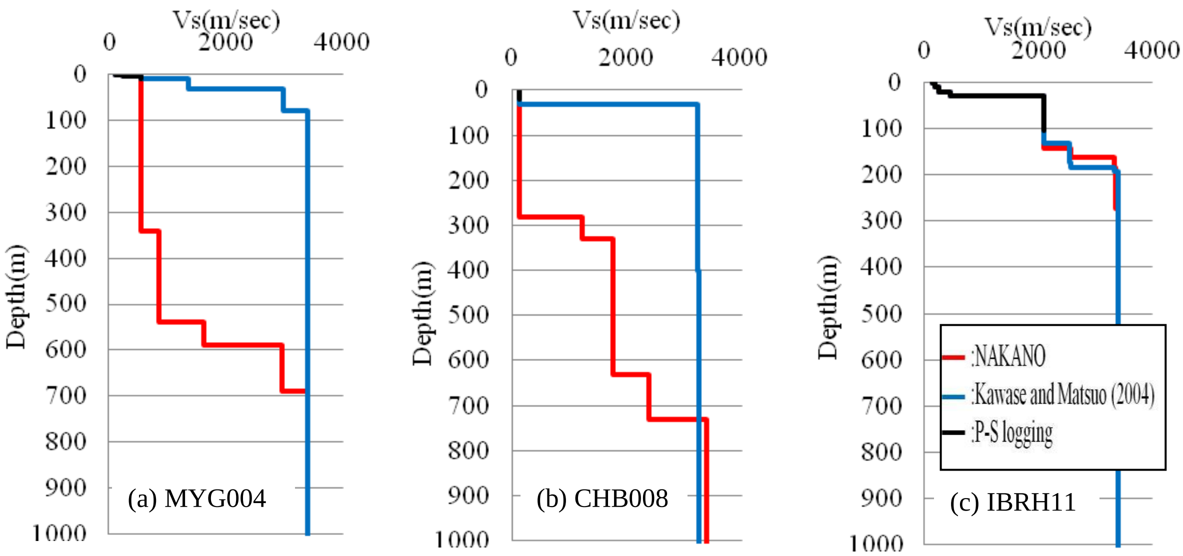

Figure 4.1. S-wave velocity structures

Thus, the significant difference between inverted S-wave velocities of our study and those of Kawase and Matsuo (2004) suggests that it is necessary to examine more carefully reliability of site factors, because a large difference would result in if separated site factors are significantly different.

5. CONCLUSION

The comparison of the inverted site factors, 1/Q and b value, M0-fc and M0-fmax relationships, stress parameter $\Delta\sigma$-M0 relationships, and S-wave velocity structures to those in the previous study led to the following conclusions:

1. Although there are differences in the site factors at some sites between our study and the previous one by Kawase and Matsuo (2004), primarily the validity of our analysis was suggested since site factors estimated by the spectral inversion and average site factors backwardly calculated by using the source factors and path effects are in good agreement.

2. The 1/Q and *b* values as path attenuation characteristics are more stable than those by Kawase and Matsuo (2004), and linear decline of 1/Q in proportion to frequency was pervasively observed.

3. There was no significant difference in M0-fc and M0-fmax relationships between our results and those of Kawase and Matsuo (2004).

4. The $\Delta\sigma$-M0 relationships has also no significant difference in between ours and Kawase and Matsuo (2004) except for Type C. In Type C, crustal earthquakes, the scale dependence of stress parameters is higher in our result than in Kawase and Matsuo (2004), however, we need careful scrutiny if this difference is statistically meaningful or not.

From the above observation, we can conclude that the validity of our spectral inversion is confirmed. We continue to study the validity of calculation and then we expand our analysis to response spectra for practical applications.

ACKNOWLEDGEMENT
We appreciate that we are allowed to use the data observed and collected by National Research Institute for Earth Science and Disaster Prevention (NIED) as well as Japan Meteorological Agency (JMA). This research was partially supported by JSPS and NSF under the Japan-U.S. Cooperative Science Program from 2011~2012 (P.I. Hiroshi Kawase, DPRI, Kyoto Univ.) and MEXT Grant-in-Aid for Scientific Research (A) No.21241044, 2009~2012 (P.I. Hiroshi Kawase, DPRI, Kyoto Univ.).

REFERENCES

Aki, K. and Richards, P., G. (2009). Quantitative Seismology, 2nd edition, University Science Books.

Andrews, D. J. (1982): Separation of Source and Propagation Spectra of Seven Manmmoth Lakes Aftershocks. Proceedings of Workshop 16, Dynamic Characteristics of Fault, *U. S. Geological Survey Open File Report*, 82-591, USGS, pp.437.

Boore, D.M.(Boore, D.M. and Atkinson, G.M. (2008). Ground-Motion Prediction Equationsfor the Average Horizontal Component of PGA, PGV, and 5%-Damped PSA at Spectral Periods between 0.01 s and 10.0 s. *Earthquake Spectra*, **Vol 24, No. 1**, 99–138.

Kanno, T., Narita, A., Morikawa, N., Fujiwara, H., and Fukushima, Y. (2006). A New Attenuation Relation for Strong Ground Motion in Japan Based on Recorded Data. *Bulletin of the Seismological Society of America*, **Vol 96, No. 3.** 879-897.

Kawase, H., Ito, S., and Kuhara, H. (2000). Strong Motion Prediction for Fukuoka City based on Distinctive Asperities and Statistical Green's Functions. *Proceedings of 6th International Conference on Seismic Zonation*, Palm Springs, California, CD-ROM, pp.6.

Kawase, H., and Matsuo, H. (2004a). Separation of Source, Path, and Site Effects based on the Observed Data by K-NET, KiK-net, and JMA Strong Motion Network. *Journal of Japan Association for Earthquake Engineering*. **Vol.4**, **No.1**, 33-52 (in Japanese with English abstract).

Kawase, H. and Matsuo, H. (2004b). Relationship of S-wave Velocity Structures and Site Effects Separated from the Observed Strong Motion Data of K-NET, KiK-net, and JMA Network. *Journal of Japan Association for Earthquake Engineering*. **Vol.4**, **No.4**, 126-145 (in Japanese with English abstract).

Kawase, H. (2006). Site Effects Derived from Spectral Inversion Method for K-NET, KiK-net, and JMA Strong-Motion Network with Special Reference to Soil Nonlinearity in High PGA Records. *Bulletin of the Earthquake Research Institute, University of Tokyo*. 81 (3/4), 309-315.

Scasserra, G., Jonathan, P.S, Bazzurro, P., Lanzo, G., and Mollaioli, F. (2009). A Comparison of NGA Ground-Motion Prediction Equations to Italian Data. *Bulletin of the Seismological Society of America*. **Vol. 99, No. 5,** 2961–2978.